Cosmological Weak Lensing and Dark Matter Mapping with the Hubble Space Telescope

Tim Schrabback[1,2], Patrick Simon[3,1], Thomas Erben[1], Peter Schneider[1], Jan Hartlap[1], Catherine Heymans[4], Phil Marshall[5,6], Hendrik Hildebrandt[1], Chris Fassnacht[7], Eric Morganson[5], Maruša Bradač[5,6], Marco Hetterscheidt[1], Tim Eifler[1], Joan-Marc Miralles[8,9,1], Jörg Dietrich[9], Robert Fosbury[10], Wolfram Freudling[10], and Norbert Pirzkal[10,11]

[1]*Argelander-Institut für Astronomie, Universität Bonn, Auf dem Hügel 71, D-53121 Bonn, Germany;* [2]*Leiden Observatory, PO Box 9513, NL-2300 RA, Leiden, the Netherlands, Email: schrabback@strw.leidenuniv.nl;* [3]*Institute for Astronomy, University of Edinburgh, Royal Observatory, Blackford Hill, Edinburgh EH9-3HJ, UK;* [4]*University of British Columbia, Department of Physics and Astronomy, 6224 Agricultural Road, Vancouver, Canada;* [5]*Kavli Institute for Particle Astrophysics and Cosmology, P.O. Box 20450, MS29, Stanford, CA 94309, USA;* [6]*Physics department, University of California, Santa Barbara, CA 93106, USA;* [7]*Department of Physics, University of California, 1 Shields Avenue, Davis, CA 95616, USA;* [8]*Tècniques d'Avantguarda, Avda. Carlemany 75, Les Escaldes, AD-700 Principat d'Andorra;* [9]*European Southern Observatory, Karl-Schwarzschild-Str. 2, D-85741 Garching, Germany;* [10]*ST-ECF, European Southern Observatory, Karl-Schwarzschild Str. 2, 85741 Garching, Germany;* [11]*Space Telescope Science Institute, 3700 San Martin Drive, Baltimore, MD 21218, USA*

Cosmological weak lensing, the gravitational lensing effect of large-scale structure, provides a unique tool to study the large-scale matter distribution and constrain the power spectrum of matter fluctuations free of assumptions on the relation between luminous and dark matter. Due to the weakness of cosmological shear, it can only be detected statistically requiring accurate correction for systematic effects, most importantly the image point-spread-function. Here we present results from our cosmological weak lensing analysis of archival data from the Advanced Camera for Surveys on board the Hubble Space Telescope. Compared to ground-based observations the excellent resolution obtained from space provides a much higher number density of resolved galaxies which can be used to extract the shear signal. This enables us to locally suppress the shape noise induced by the intrinsic ellipticities of galaxies, which is particularly useful for dark matter mapping and constraining the small-scale power spectrum. He have already completed a pilot study using early data from the ACS Parallel Cosmic Shear Survey and the combined GEMS and GOODS mosaic of the *Chandra* Deep Field South (CDFS). From the low shear signal detected in the GEMS/GOODS data we conclude that this field is subject to strong sampling variance, with an exceptional under-density in its foreground. In a preliminary analysis of the HST/COSMOS Survey we detect residual systematics at small angular scales, whose origin is currently been investigated. Using only B-mode-free scales we find a preliminary estimate for the normalisation of the matter fluctuation power spectrum $\sigma_8 = 0.71 \pm 0.09$ (68% confidence) for a matter density $\Omega_{\rm m} = 0.24$, where the error includes the uncertainties in the redshift distribution, the Hubble constant, and the shear calibration, as well as a Gaussian estimate for cosmic variance.

Keywords: Cosmology, gravitational lensing, large-scale structure

1. Introduction

Gravitational lensing describes the deflection and distortion of light bundles in the gravitational potential of foreground matter concentrations. This effect can be described as a straightforward application of General Relativity. Hence, it provides a tool to study the total (mostly dark) foreground matter distribution free of assumptions on the relative distribution of luminous and dark matter. Some galaxy clusters are sufficiently massive to create prominent strong lensing features such as multiply-imaged background galaxies, with angular positions near the line-of-sight to the cluster (Fig. 1). However, the images of most galaxies on the sky are only weakly distorted by the projected tidal gravitational field of the typically less concentrated matter inhomogeneities of large-scale structure. Due to the intrinsic ellipticities of galaxies, these distortions cannot be detected from individual galaxies (for which a typical shear-signal-to-noise is of order $\sim 1/30$), but only from an ensemble of coherently lensed galaxies. Measuring the lensing effect of large-scale structure, which is termed *cosmic shear* or *cosmological weak lensing*, provides a powerful tool to study the power spectrum of the total matter fluctuations, so far yielding constraints on the matter content $\Omega_{\rm m}$ and the power spectrum normalisation σ_8, see Ref. 1 for a compilation of recent values and Refs. 2–6 for reviews. Recently Ref. 7 presented a joint analysis from the CFHTLS-Wide, RCS, VIRMOS-DESCART, and GaBoDS surveys, amounting to a total sky area of $\sim 100\,\mathrm{deg}^2$, from which they find $\sigma_8(\Omega_{\rm m}/0.24)^{0.59} = 0.84 \pm 0.05$. If accurate (photometric) redshifts are available for the source galaxies, the evolution of the shear signal can be constrained, which is a sensitive test to discriminate between different dark energy models due to its dependencies on structure growth and the involved distance ratios,[8,9] see Refs. 10–13 for first constraints on the dark energy equation-of-state parameter w.

Due to the weakness of cosmological shear, proper correction for systematic effects, first of all the image point-spread-function (PSF) is indis-

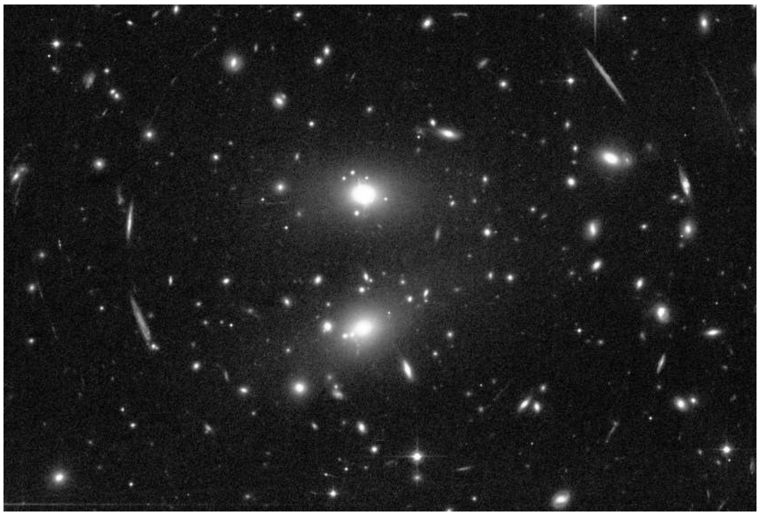

Fig. 1. HST/ACS image of the central region of the galaxy cluster RXJ1347–1145. Besides the bright cluster members many background galaxies are visible, whose images are highly distorted by the tidal gravitational field of the cluster. In the case of cosmological weak lensing the distortions are typically much weaker and can only be detected statistically (Image credit: NASA/ESA/AIfA; Erben/Schrabback).

pensable. The PSF dilutes the shear signal by isotropic blurring and creates spurious signal due to anisotropy, which can easily exceed the cosmological signal. A precise correction is particularly important in view of the next generation of cosmic shear surveys, which will provide the statistical power to measure cosmological shear with percent and sub-percent level accuracy aiming at precision measurements of dark energy properties. This will only be possible if the methods used to extract the shear signal by measuring galaxy shapes from noisy and PSF-distorted images have a comparable systematic accuracy. In order to assess the accuracy of existing methods and to provide a platform for further development, the Shear TEsting Programme[a] (STEP) was launched in 2004. So far blind analyses of simulated images containing a hidden shear signal have been conducted.[14,15] These benchmarks show that several shape measurement techniques already reach an average relative systematic accuracy of a few percent, which is sufficient for current studies, but substantial development is still required for future surveys. Important progress has also been made in the development of diag-

[a]`http://www.physics.ubc.ca/~heymans/step.html`

nostic tools for the detection of residual systematics, such as the E-/B-mode decomposition,[16,17] where the curl B-mode cannot be created by lensing, and the galaxy-star cross-correlation.[18]

Most of the ongoing and planned weak lensing surveys use ground-based wide-field imaging data. These are hampered by image blurring (seeing) due to atmospheric turbulence which erases the shear information for unresolved galaxies limiting the number density of usable galaxies to $\lesssim 30/\mathrm{arcmin}^2$. The disturbing influence of Earth's atmosphere can be avoided by using space-based images, which provide a higher number density of resolved background sources and better control for systematics on the cost of smaller sky coverage. The higher number density obtained from space helps to locally beat down the shape noise induced by the intrinsic ellipticities of the source galaxies. This is particularly important in order to constrain the small-scale power spectrum and reconstruct the projected matter distribution. In these proceedings we summarise results from our ongoing cosmological weak lensing analysis of archival data from the *Advanced Camera for Surveys* (ACS) on board the *Hubble Space Telescope* (HST), providing the currently largest set of data suitable for space-based cosmic shear measurements. Combining a relatively large field-of-view ($3'.3 \times 3'.3$) with high sensitivity (48% total throughput at 660 nm), good PSF-sampling ($0''.05$ per pixel) and space-based resolution ($\sim 0''.10$ at 800 nm), HST/ACS was the best instrument for weak lensing measurements at small angular scales until its unfortunate loss on January 27th, 2007.

2. Practical concerns for measuring weak lensing with ACS

Before being able to use the ACS data for weak lensing studies, it was necessary to develop several technical tools and carefully test our weak lensing pipeline:

Firstly, we developed an image reduction pipeline for ACS data, which fulfils the strict requirements weak lensing places on the data quality, e.g. regarding careful image registration and bad pixel masking.

Secondly, the detection of strong temporal variations of the ACS PSF (Fig. 2), which are interpreted as focus changes due to thermal breathing of the telescope, led to the development of a new PSF correction scheme. Classically, PSF variations across the field-of-view are modelled by interpolating measured stellar shape parameters using polynomial functions. However, due to the small field-of-view of ACS, high galactic latitude fields contain only of order 10 stars, which are too few for a direct interpolation. In our correction scheme we fit the stars present in a galaxy field with PSF

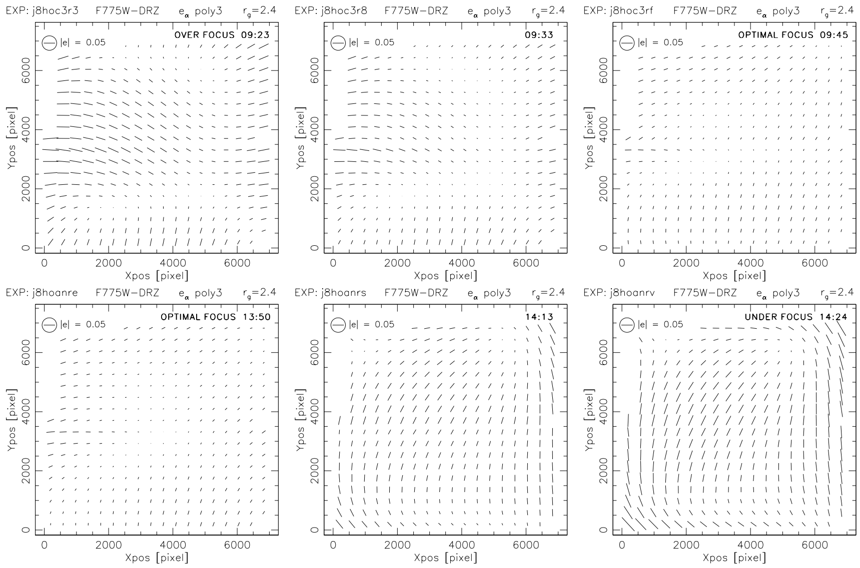

Fig. 2. Third-order polynomial fits to stellar ellipticities in the drizzled images of two series of subsequent ACS/WFC exposures, where the bars indicate the ellipticity of the PSF. The 400 second exposures were taken on 2002-08-28 (*upper* panels) and 2002-08-17 (*lower* panels), where the time indicated corresponds to the middle of the exposure (UT). The variations are interpreted as thermal breathing of the telescope. The *upper right* and *lower left* plots are near the optimal focus position, whereas the other exposures represent positive focus offsets (*upper left* panel) or negative focus offsets (*lower right* panel). Figure taken from Ref. 19.

models derived from dense stellar fields. We determine the correction on the basis of single exposures in order to obtain an optimal time-dependence of the solution and exclude noise in the ellipticity measurement caused by resampling. We apply a principal component analysis (PCA) to the polynomial interpolation coefficients of the PSF anisotropy kernel[19,20] (a PSF-width-scaled version of the PSF ellipticity) computed for several hundred stellar field exposures of different ACS broad-band filters. From the PCA we find that indeed most of the PSF variation ($\sim 60\%$ of the variance) occurs in a one-dimensional parameter space, which can be related to the focus position (Fig. 3). We estimate that our PSF correction scheme reduces the systematic contribution to the shear correlation functions due to PSF distortions to $< 2 \times 10^{-6}$ for galaxy fields containing at least 10 stars.[19] This corresponds to $\lesssim 5\%$ of the cosmological signal expected on scales of a single ACS field.

Thirdly, we carefully tested our weak lensing pipeline, which is based on

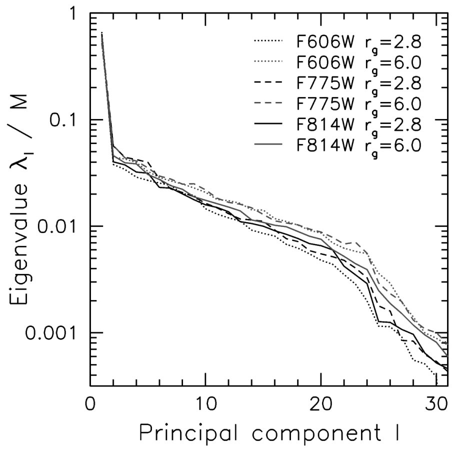

Fig. 3. Normalised eigenvalues λ_l/M for the first 30 principal components of the temporal variation of the ACS PSF polynomial coefficients. The normalised eigenvalue of a principal component gives the relative contribution of the model variation along the direction spanned by the corresponding principal vector, relative to the total variance in coefficient space. The different curves correspond to the ACS filters F606W, F775W, and F814W and two different PSF filter scales $r_g = (2.8, 6.0)$ pixels. In all cases about 60% of the total variation occurs along the direction of the dominant first principal component, which can be related to the focus position.

the KSB-formalism,[20] using simulated images from the STEP Programme. After eliminating biases identified in the first round of simulations,[14] our pipeline performed among the most accurate methods with an average (relative) shear recovery accuracy of $\sim 2\%$ on the second simulation set.[15] It also achieves a similar average accuracy in a preliminary analysis of the third set of STEP simulations (Rhodes et al. in prep.), which features space-based weak lensing data, partially with ACS-like properties. In this test our updated pipeline also yields a good correction as a function of galaxy size and magnitude ($\sim \pm 5\%$ variation), which is important if one aims at measuring the shear signal as a function of source redshift. Concluding from STEP, the systematic accuracy of our pipeline should be well within the statistical noise of the ACS weak lensing data.

Finally, the continuous bombardment of ACS with cosmic rays creates defects in the CCDs reducing the charge-transfer efficiency (CTE). This leads to charge trails trailing behind objects in the read-out direction. In order to correct for this influence on galaxy shapes we apply a parametric correction model similar to the one proposed by Ref. 21.

3. Cosmological weak lensing analysis of the ACS archive

Our cosmological weak lensing analysis was done in two steps: In a pilot study[19] we first test the capabilities of ACS for cosmic shear measurements with early data from the ACS Parallel Survey (Sect. 3.1) and the combined GEMS and GOODS ACS mosaic of the *Chandra* Deep Field South

(CDFS, Sect. 3.2). We are currently analysing two much larger data sets, the Extended ACS Parallel Survey (Sect. 3.1) and the HST/COSMOS Survey (Sect. 3.3).

3.1. *The Extended ACS Parallel Survey*

In the pilot study[19] we use a limited set of 59 independent ACS pointings from the ACS Parallel Cosmic Shear Survey. These parallel data are taken simultaneously with primary observations with another HST camera. As the cameras point at positions separated by several arcminutes, parallel observations provide almost random pointings, which is helpful to measure a statistical quantity such as cosmological shear. Yet, due to the relatively small field-of-view of ACS, the shear correlation signal can only be measured at relatively small angular separations. In the pilot study parallel data we detect a low level of remaining systematics manifesting in a slight net alignment of the galaxies in the direction of the image y-axis. There are indications that this signal originates from the poor data quality caused by a lack of sufficient dithering of the data. We therefore developed several upgrades to our data reduction and analysis pipeline in order to reliably reject affected galaxies.

We are currently analysing a much larger data set consisting of 440 pointings or a total area of $1.22\,\mathrm{deg}^2$. Besides $\sim 69\%$ of parallel data we also add primary observations which resemble quasi-random pointings for cosmic shear, as they either target very near ($z < 0.07$) or distant ($z > 1.2$) objects with a low lensing efficiency. From this "Extended ACS Parallel Survey" we aim to constrain the small-scale power spectrum with high accuracy, which strongly depends on the largely unknown inter-play of baryons and dark matter. The analysis of this data set is done jointly with the HAGGLeS Project, which aims at the detection of galaxy-scale strong lenses in the ACS archive (Marshall et al. in prep.).

3.2. *GEMS/GOODS*

The combined GEMS and GOODS mosaic of the *Chandra* Deep Field South spans a total area of $\sim 28' \times 28'$ imaged with the ACS/WFC using the F606W filter, with an exposure time of 2.2ks for GEMS, where we use a similarly deep stack for GOODS. In Ref. 19 we perform a number of diagnostic tests indicating that the remaining level of systematics is consistent with zero for the GEMS and GOODS data confirming the success of our PSF correction scheme. Combining our shear estimate of the GEMS and GOODS observations using 96 galaxies arcmin^{-2} with the photometric redshift catalogue of the GOODS-MUSIC sample,[22] we determine a *local single field estimate* for the mass power spectrum normalisation $\sigma_8 = 0.59^{+0.13}_{-0.17}\,(\mathrm{stat}) \pm 0.07\,(\mathrm{sys})$ (68% confidence assuming Gaussian sampling variance) at a fixed matter density $\Omega_{\mathrm{m}} = 0.24$ for a ΛCDM cosmology, where we marginalise over the uncertainty of the Hubble constant and the redshift distribution. This estimate agrees only marginally with the WMAP-3 result[23] of $\sigma_8 = 0.761^{+0.049}_{-0.048}$ and is significantly below values found by recent ground-based surveys.[7] From this discrepancy we conclude that the CDFS is subject to strong sampling variance with a significant under-density of compact foreground structures. This is consistent with a recent study by Ref. 24, who find a strong deficiency of red galaxies in this field. Note that Ref. 25 originally derived a higher value $\sigma_8 = 0.79 \pm 0.15$ (for $\Omega_{\mathrm{m}} = 0.24$) from the GEMS data. While we have been able to show that their and our shear measurements agree with a relative accuracy of $\sim 3\%$, we found that their σ_8 estimate is most probably biased due to an under-estimation of the mean redshift of the survey.

Studies performing ray-tracing through N-body simulations indicate that non-linear evolution leads to significant non-Gaussian sampling variance,[26,27] which suggests that we actually under-estimate the statistical uncertainty. The frank conclusion is that the sky coverage of GEMS is too small to yield representative cosmological parameter constraints using cosmic shear. The concluding picture is that the line-of-sight in the CDFS mostly passes through voids, whereas compact structures are rare. Following from the preliminary ray-tracing comparison by Hartlap et al. (in prep.), this seems to be a peculiar, but not extraordinary rare configuration, assuming a WMAP-3 cosmology.

Note that our σ_8 estimate from the CDFS was more discrepant with other weak lensing results at the time of the analysis. For example, early results from the CFHTLS yielded significantly higher σ_8 estimates of $\sigma_8 = 0.86 \pm 0.05$[12] and $\sigma_8 = 0.85 \pm 0.06$[11] computed for $\Omega_{\mathrm{m}} = 0.3$, which corresponds to $\sigma_8 = 0.98 \pm 0.06$ and $\sigma_8 = 0.97 \pm 0.07$ for $\Omega_{\mathrm{m}} = 0.24$. However, with the new analysis by Ref. 7, which makes use of a carefully calibrated redshift distribution and considers recent STEP results, the tension has been significantly reduced. It will be interesting to observe if this trend towards lower σ_8 estimates from cosmological weak lensing studies continues in the post-STEP era.

3.3. *COSMOS*

We also conducted a preliminary analysis of the HST/COSMOS Survey. Although this is also a single mosaic field, the approximately seven times larger sky area of 1.64 deg^2 considerably reduces the influence of sampling variance compared to GEMS. From our analysis we have been able to confirm the main features of the projected dark matter maps found by Ref. 28. The maps show several mass peaks associated with galaxy clusters and groups, partially connected with filamentary structures (see Fig. 4). In addition, a huge relatively empty region is visible in the lower right (south-west) quadrant of the mosaic, with a diameter $\gtrsim 25h^{-1}$ Mpc at a typical lens redshift $z \sim 0.4$ (assuming a flat ΛCDM cosmology). We expect that this line-of-sight has similar statistical properties as the GEMS Survey, being a projecting of mostly voids along the line-of-sight, but we did not test this quantitatively.

From the COSMOS data we have been able to measure the cosmic shear signal at a wide range of scales $0\farcm1 \lesssim \theta \lesssim 80'$. At small scales we detect a significant B-mode signal (curl-component) indicating remaining uncorrected systematics (Fig. 5), where the affected scales are $\theta \lesssim 0\farcm7$ for the shear two-point correlation function and $\theta \lesssim 5'$ for the dispersion of the aperture mass statistics.[30] The spurious B-mode signal might be related to residuals of the PSF correction, but this is still under investigation. Similar indications for remaining systematics have been reported by Ref. 31 for their analysis of the data. We perform a preliminary cosmological parameter estimation, in which we only use B-mode free scales ($\theta > 1'$ for the shear two-point correlation function), and a redshift distribution based on the public redshift catalogue by Ref. 32. From the COSMOS data we obtain an estimate for the power spectrum normalisation $\sigma_8 = 0.71 \pm 0.09$ (68% confidence) for $\Omega_\mathrm{m} = 0.24$, where the error includes the uncertainties in the redshift distribution, the Hubble constant, and the shear calibration, as well as a Gaussian estimate for cosmic variance. This result is in excellent agreement with the WMAP-3 result of $\sigma_8 = 0.761^{+0.049}_{-0.048}$. Yet, our estimate agrees only marginally with recent ground-based estimates, which favour slightly higher values of σ_8. However, the fact that no extraordinarily massive galaxy cluster is present in the field at redshifts with high lensing efficiency might suggest a σ_8 estimate rather at the low end of the expected range. Thus, we find it surprising that our measurement differs significantly from the estimate by Ref. 31 for the same field, who find $\sigma_8 = 0.90 \pm 0.083\,(\mathrm{stat.}) \pm 0.104\,(\mathrm{syst.})$ from a similar analysis using one redshift bin and $\sigma_8 = 0.96 \pm 0.037\,(\mathrm{stat.})^{+0.058}_{-0.039}\,(\mathrm{syst.})$ from a tomo-

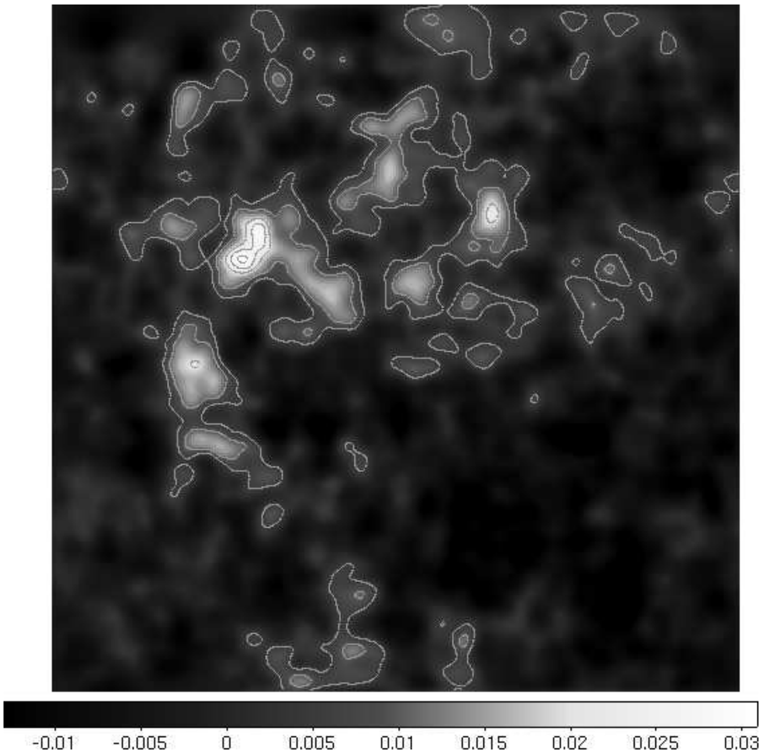

Fig. 4. Maximum likelihood reconstruction of the convergence κ (projected mass) in the COSMOS field from our shear catalogue applying noise propagation and Wiener filtering.[29] The absolute scale has been set such that the mean κ vanishes. The contours start at and are spaced in steps of $\kappa = 0.005$. Note that we use less galaxies due to our more stringent selection criteria ($43/\mathrm{arcmin}^2$) compared to the independent analysis by Ref. 28, leading to a larger effective smoothing scale of our map.

graphic analysis using three bins, both for $\Omega_{\rm m} = 0.24$. Note that differences within the statistical and systematic errors are not unexpected, given that independent data reduction and shear measurement pipelines have been applied, as well as different selection criteria. Yet, their tomographic results and our estimate are clearly not consistent. So far we have not been able to unambiguously identify the origin for this discrepancy. However, note that both catalogues still contain indications for systematic at small scales. Once these are eliminated by further improvements in the PSF correction and analysis scheme, the discrepancy might partially resolve.

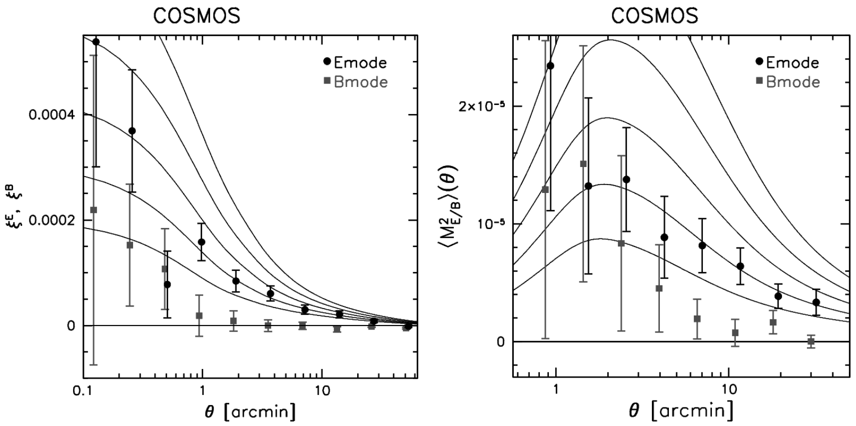

Fig. 5. E/B-mode decomposition of our COSMOS analysis using the shear correlation functions (left) and the dispersion of the aperture mass (right). While the E-mode signal can be created both by lensing and systematics, the B-mode must be due to systematics. It is therefore likely, that at small scales, where a significant B-mode is detected, also the E-mode signal will be affected by systematics. Thus, only the large, B-mode-free scales can be used for a cosmological parameter estimation. The curves indicate ΛCDM predictions for $\Omega_{\rm m} = 0.3$ and $\sigma_8 = (0.6, 0.7, 0.8, 0.9, 1.0)$. For the decomposition using the correlation function an extrapolation of the shear signal to infinity is required, for which we assume $\sigma_8 = 0.7$. The error-bars include the uncertainty due to shape noise but not cosmic variance.

4. Conclusions

We found that the ACS PSF varies on short time scales, which is properly taken into account in our PSF correction scheme. From the analysis of the GEMS and GOODS data we conclude that the CDFS is an exceptionally under-dense field. Hence, although it is one of the best-studied fields in the sky, it cannot be considered to be fully representative for the cosmic mean. In our preliminary analysis of the HST/COSMOS data we recover the main structures in the dark matter maps by Ref. 28 with good consistency, which show that baryons trace the distribution of dark matter well on large scales. Our preliminary cosmological parameter estimation from COSMOS yields $\sigma_8 = 0.71 \pm 0.09$ consistent with WMAP3, but significantly below the value found by Ref. 31. However, note that our analysis is only preliminary as we still detect indications for remaining systematics, which we hope to eliminate with an upgraded analysis and correction scheme. A very interesting comparison will be possible with the Extended ACS Parallel Survey, which is expected to yield tight constraints on the cosmic shear signal at small angular scales, possibly providing interesting insights into the interplay of dark matter and baryons on scales of ~ 100 kpc.

Cosmological weak lensing studies with ACS, such as the one presented here, but also the work by Refs. 21,25,31,33,34 play a pathfinder role for dedicated future cosmic shear missions from space such as DUNE or JDEM/SNAP: Not only acting as proof of concept for envisaged future projects, they also provide first estimates for the small-scale signal, which can be used as input to estimate the accuracy of future studies. Furthermore, current projects with ACS yield substantial technical expertise, which will be very valuable for the planning, conduction, and analysis of future surveys. Following from the experience with ACS future mission should for example aim to achieve maximal thermal stability to minimise temporal variations of the point-spread-function. Also, it will be crucial to use hardened CCD chips, which are subject to less CTE degradation. Concerning the analysis of future surveys, tools such as our PSF interpolation scheme, possibly upgraded using a principal component analysis, will be very valuable to achieve the systematic accuracy sought.

In general cosmological weak lensing is currently developing into a mature field of cosmology, which will yield precision constraints on the power spectrum, dark matter, and dark energy with the coming surveys.

References

1. M. Hetterscheidt, P. Simon, M. Schirmer, H. Hildebrandt, T. Schrabback, T. Erben and P. Schneider, *A&A* **468**, 859(June 2007).
2. M. Bartelmann and P. Schneider, *Phys. Rep.* **340**, p. 291 (2001).
3. Y. Mellier, L. van Waerbeke, E. Bertin, I. Tereno and F. Bernardeau, Wide-field cosmic shear surveys, in *Astronomical Data Analysis II. Edited by Starck, Jean-Luc; Murtagh, Fionn D. Proceedings of the SPIE, Volume 4847, pp. 112-122 (2002).*, December 2002.
4. H. Hoekstra, H. K. C. Yee and M. D. Gladders, *New Astronomy Review* **46**, 767(November 2002).
5. A. Refregier, *ARA&A* **41**, 645 (2003).
6. P. Schneider, C. S. Kochanek and J. Wambsganss, *Saas-Fee Advanced Course 33: Gravitational Lensing: Strong, Weak and Micro* (Springer Verlag, Berlin, 2006).
7. J. Benjamin, C. Heymans, E. Semboloni, L. Van Waerbeke, H. Hoekstra, T. Erben, M. D. Gladders, M. Hetterscheidt, Y. Mellier and H. K. C. Yee, *MNRAS accepted (also astro-ph/0703570)* (March 2007).
8. J. Peacock, P. Schneider, G. Efstathiou, J. Ellis, B. Leibundgut, S. Lilly and Y. Mellier, *http://www.stecf.org/coordination/esa_eso/cosmology.php* (September 2006).
9. A. Albrecht, G. Bernstein, R. Cahn, W. L. Freedman, J. Hewitt, W. Hu, J. Huth, M. Kamionkowski, E. W. Kolb, L. Knox, J. C. Mather, S. Staggs

and N. B. Suntzeff, *astro-ph/0609591* (September 2006).
10. M. Jarvis, B. Jain, G. Bernstein and D. Dolney, *ApJ* **644**, 71(June 2006).
11. H. Hoekstra, Y. Mellier, L. van Waerbeke, E. Semboloni, L. Fu, M. J. Hudson, L. C. Parker, I. Tereno and K. Benabed, *ApJ* **647**, 116(August 2006).
12. E. Semboloni, Y. Mellier, L. van Waerbeke, H. Hoekstra, I. Tereno, K. Benabed, S. D. J. Gwyn, L. Fu, M. J. Hudson, R. Maoli and L. C. Parker, *A&A* **452**, 51(June 2006).
13. T. D. Kitching, A. F. Heavens, A. N. Taylor, M. L. Brown, K. Meisenheimer, C. Wolf, M. E. Gray and D. J. Bacon, *MNRAS* , 138(April 2007).
14. C. Heymans, L. Van Waerbeke, D. Bacon, J. Berge, G. Bernstein, E. Bertin, S. Bridle, M. L. Brown, D. Clowe, H. Dahle, T. Erben, M. Gray, M. Hetterscheidt, H. Hoekstra, P. Hudelot, M. Jarvis, K. Kuijken, V. Margoniner, R. Massey, Y. Mellier, R. Nakajima, A. Refregier, J. Rhodes, T. Schrabback and D. Wittman, *MNRAS* **368**, 1323(May 2006).
15. R. Massey, C. Heymans, J. Bergé, G. Bernstein, S. Bridle, D. Clowe, H. Dahle, R. Ellis, T. Erben, M. Hetterscheidt, F. W. High, C. Hirata, H. Hoekstra, P. Hudelot, M. Jarvis, D. Johnston, K. Kuijken, V. Margoniner, R. Mandelbaum, Y. Mellier, R. Nakajima, S. Paulin-Henriksson, M. Peeples, C. Roat, A. Refregier, J. Rhodes, T. Schrabback, M. Schirmer, U. Seljak, E. Semboloni and L. van Waerbeke, *MNRAS* **376**, 13(March 2007).
16. R. G. Crittenden, P. Natarajan, U.-L. Pen and T. Theuns, *ApJ* **568**, 20(March 2002).
17. P. Schneider and M. Kilbinger, *A&A* **462**, 841(February 2007).
18. D. J. Bacon, R. J. Massey, A. R. Refregier and R. S. Ellis, *MNRAS* **344**, 673(September 2003).
19. T. Schrabback, T. Erben, P. Simon, J.-M. Miralles, P. Schneider, C. Heymans, T. Eifler, R. A. E. Fosbury, W. Freudling, M. Hetterscheidt, H. Hildebrandt and N. Pirzkal, *A&A* **468**, 823(June 2007).
20. N. Kaiser, G. Squires and T. Broadhurst, *ApJ* **449**, p. 460 (1995).
21. J. D. Rhodes, R. J. Massey, J. Albert, N. Collins, R. S. Ellis, C. Heymans, J. P. Gardner, J.-P. Kneib, A. Koekemoer, A. Leauthaud, Y. Mellier, A. Refregier, J. E. Taylor and L. Van Waerbeke, *ApJS* **172**, 203(September 2007).
22. A. Grazian, A. Fontana, C. de Santis, M. Nonino, S. Salimbeni, E. Giallongo, S. Cristiani, S. Gallozzi and E. Vanzella, *A&A* **449**, 951(April 2006).
23. D. N. Spergel, R. Bean, O. Doré, M. R. Nolta, C. L. Bennett, J. Dunkley, G. Hinshaw, N. Jarosik, E. Komatsu, L. Page, H. V. Peiris, L. Verde, M. Halpern, R. S. Hill, A. Kogut, M. Limon, S. S. Meyer, N. Odegard, G. S. Tucker, J. L. Weiland, E. Wollack and E. L. Wright, *ApJS* **170**, 377(June 2007).
24. S. Phleps, C. Wolf, J. A. Peacock, K. Meisenheimer and E. van Kampen, *A&A* **468**, 113(June 2007).
25. C. Heymans, M. L. Brown, M. Barden, J. A. R. Caldwell, K. Jahnke, C. Y. Peng, H.-W. Rix, A. Taylor, S. V. W. Beckwith, E. F. Bell, A. Borch, B. Häußler, S. Jogee, D. H. McIntosh, K. Meisenheimer, S. F. Sánchez, R. Somerville, L. Wisotzki and C. Wolf, *MNRAS* **361**, 160(July 2005).
26. M. Kilbinger and P. Schneider, *A&A* **442**, 69(Octtober 2005).

27. E. Semboloni, L. van Waerbeke, C. Heymans, T. Hamana, S. Colombi, M. White and Y. Mellier, *MNRAS* **375**, L6(February 2007).
28. R. Massey, J. Rhodes, R. Ellis, N. Scoville, A. Leauthaud, A. Finoguenov, P. Capak, D. Bacon, H. Aussel, J.-P. Kneib, A. Koekemoer, H. McCracken, B. Mobasher, S. Pires, A. Refregier, S. Sasaki, J.-L. Starck, Y. Taniguchi, A. Taylor and J. Taylor, *Nature* **445**, 286(January 2007).
29. W. Hu and C. R. Keeton, *Phys. Rev. D* **66**, 063506(September 2002).
30. P. Schneider, L. van Waerbeke, B. Jain and G. Kruse, *MNRAS* **296**, 873(June 1998).
31. R. Massey, J. Rhodes, A. Leauthaud, P. Capak, R. Ellis, A. Koekemoer, A. Réfrégier, N. Scoville, J. E. Taylor, J. Albert, J. Bergé, C. Heymans, D. Johnston, J.-P. Kneib, Y. Mellier, B. Mobasher, E. Semboloni, P. Shopbell, L. Tasca and L. Van Waerbeke, *ApJS* **172**, 239(September 2007).
32. B. Mobasher, P. Capak, N. Z. Scoville, T. Dahlen, M. Salvato, H. Aussel, D. J. Thompson, R. Feldmann, L. Tasca, O. Lefevre, S. Lilly, C. M. Carollo, J. S. Kartaltepe, H. McCracken, J. Mould, A. Renzini, D. B. Sanders, P. L. Shopbell, Y. Taniguchi, M. Ajiki, Y. Shioya, T. Contini, M. Giavalisco, O. Ilbert, A. Iovino, V. Le Brun, V. Mainieri, M. Mignoli and M. Scodeggio, *ApJS* **172**, 117(September 2007).
33. A. Leauthaud, R. Massey, J.-P. Kneib, J. Rhodes, D. E. Johnston, P. Capak, C. Heymans, R. S. Ellis, A. M. Koekemoer, O. Le Fèvre, Y. Mellier, A. Réfrégier, A. C. Robin, N. Scoville, L. Tasca, J. E. Taylor and L. Van Waerbeke, *ApJS* **172**, 219(September 2007).
34. M. J. Jee, J. P. Blakeslee, M. Sirianni, A. R. Martel, R. L. White and H. C. Ford, *PASP accepted (also astro-ph/0710.5560)* **710**(Octtober 2007).